

20 Story Steel Buildings Equipped with Viscous Fluid Dampers Optimized in Placement Considering P-Delta Dynamic Analysis and Soil-Structure Interaction

¹Pham Nhan Hoa, ²Chu Quoc Thang, ³Hoàng Công Duy

¹Department of Civil Engineering, International University - Vietnam National University - HCM and Faculty of Civil Engineering and Applied Mechanics, HCMC University of Technology and Education, 1 Vo Van Ngan Street, Thu Duc District, Ho Chi Minh City, Vietnam.

²Department of Civil Engineering, International University - Vietnam National University – HCM.

³Faculty of Engineering and Technology, Quy Nhon University.

E-mail: pnhoa@hcmiu.edu.vn or 1421003@student.hcmute.edu.vn, cqthang@hcmiu.edu.vn, hcduy@ftt.edu.vn

ABSTRACT

The paper presents an approach to determine dynamic response of a twenty-story steel building which is retrofitted with viscous fluid dampers (VFD) of the superstructure and employs two kinds of pile-foundations. This dynamic analysis is related to all P-Δ effect, soil-structure interaction (SSI), and the simplified sequential search algorithm (SSSA). The numerical example illustrates differences of linear versus P-Δ, Non-SSI versus SSI, Non-VFD controlled versus VFD controlled, and No-SSSA versus SSSA analysis for the building subject to seismic loading. These differences shown in the conclusion help structural designers for earthquake resistance.

Keywords: Dynamics of Structures, Structural Control, P-Delta analysis, Viscous Fluid Dampers, Soil-structure Interaction, Simplified Sequential Search Algorithm

1. INTRODUCTION

Subjected to seismic, wind, other types of transient shock, to achieve optimal performance, a structure using dampers with passive control is one of the efficient ways. By retrofitting fluid viscous dampers (VFD), the energy input from a transient such as earthquake excitations is dissipated by the structure and the supplemental. If choosing reasonable damping parameters in VFD, VFD are one of most useful passive devices thank to its reasonable and economy [4][5][22].

The finite element method (FEM) with linear dynamic analysis does not consider effect of axial forces on incremental moments in a beam-column. Through stability functions, an axial force in a beam-column are embedded to its flexural stiffness matrix [6][7][8][9][10][11]. Therefore, both p-delta and P-Δ effects in a VFD structure are considered more thoroughly.

The Simplified Sequential Search Algorithm (SSA) is proposed in [28]. This procedure finds the optimal placement of VFD dampers with linear analysis. Based on the linear analysis, one by one VFD is placed in the portal of a structure where two ends of a VFD is maximized. The procedure does not consider P-Δ effects and whether it was true for high-rise buildings where axial forces in columns at the first floor are significant to their moment.

The papers [15][16] propose a set of formulas for dynamic stiffness of a pile-soil system in a layered elastic continuum. For two-layerd soil, dynamic stiffness of a pile-foundation can be determined as [19]. With the researches, a pile-foundation could be reduced as lump parameter models. Accompanied with superstructure dynamic analysis of soil-structure interaction is conducted more accurately.

2. THE MODEL OF VFD STRUCTURES CON P-DELTA AND SSI ANALYSIS

2.1 Computational Model

Consider the m -bay, n -story planar frame and its pile foundation beneath two soil-layers shown as Figure 1. The structure has VFD quantity of $(m \times n)$ VFD equipment at each of the portals. The external forces consist of lateral x , y axis forces and moment P^x, P^y, M at one node accompanied with a horizontally and vertically excited earthquake loadings \ddot{x}_g, \ddot{y}_g .

Flexural stiffness of elements depend on their $EI_{j,i}^b, EI_{j,i}^c$ length $L_{j,i}$, and particularly axial internal forces $N_{j,i}$. The stiffness matrix of P-Delta is obtained as [11]. Hence, the matrix is not constant like dynamic linear analysis but varies arbitrarily in time. The element internal axial forces are governed by their mass-accelerations, damping-velocities, and stiffness-displacements.

A damping force vector generated by a VFD is determined by using its velocities at two ends and expressed as [4]

$$\left| F_{i,j}^{VFD} = C_{i,j}^{VFD} \left| \dot{x}_{i,j}^{\otimes} - \dot{x}_{i,j}^{\ominus} \right|^{\alpha_{i,j}^{VFD}} \text{sign} \left(\dot{x}_{i,j}^{\otimes} - \dot{x}_{i,j}^{\ominus} \right) \right| \leq F_{i,j}^{\max} \quad (1)$$

where $C_{i,j}^{VFD}$ and α are damping and power coefficients, respectively. A maximum VFD damper force $F_{i,j}^{VFD}$ derives from the manufacture [5]. $(\dot{x}_{i,j}^{\otimes} - \dot{x}_{i,j}^{\ominus})$ is subtraction of two end velocities.

http://www.ejournalofscience.org

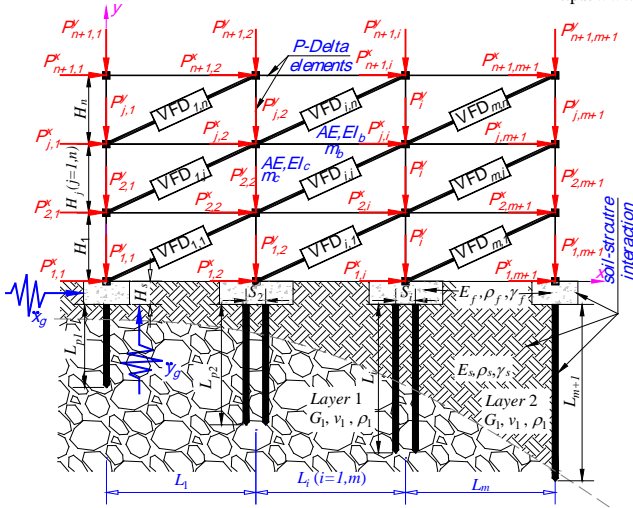


Figure 1: A VFD structure with P-delta and SSI analysis

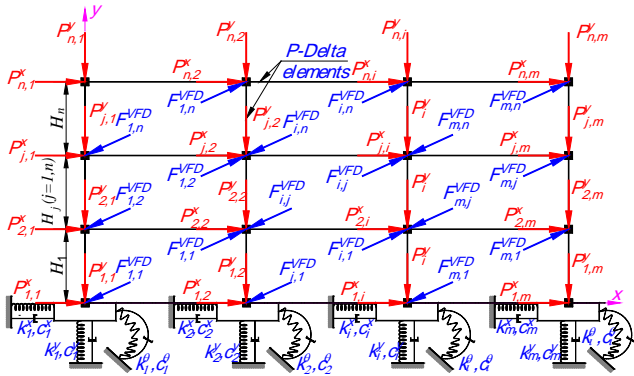


Figure 2: Mathematical model for the structure

Dynamic stiffnesses (k_i, c_i) [19][20] along x, y -axes, and about z -axis of in SSI of a pile-foundation are determined from the pile-cap, pile dimensions, distances among the piles, as well as the foundation material properties, dynamic properties E_s, ρ_s, c_s of soil enveloping the foundation. The dynamic stiffnesses are also influenced by the number of soil layers containing the piles. Equation of motion for a VFD building considering SSI is presented as

$$\mathbf{M}\ddot{\mathbf{u}} + \mathbf{C}\dot{\mathbf{u}} + \mathbf{K}\mathbf{u} = \mathbf{P} - \mathbf{M}\mathbf{1}\ddot{\mathbf{u}}_g - \mathbf{F}_{\text{VFD}} \quad (2)$$

where \mathbf{M} is a lump mass matrix including the mass of the superstructure \mathbf{M}_{CnB} and of pile-foundation \mathbf{M}_{SSI} . \mathbf{K} is a stiffness matrix including the stiffness of the superstructure \mathbf{K}_{CnB} determined as [1] and \mathbf{K}_{SSI} determined as [12][15]; and \mathbf{C} is the damping matrix including the damping matrix of the superstructure computed using the Rayleigh formula as [2] and the damping of pile-foundation determined from [19]. \mathbf{u} is a displacement vector; $\dot{\mathbf{u}} = \frac{d}{dt}\mathbf{u}$ and $\ddot{\mathbf{u}} = \frac{d^2}{dt^2}\mathbf{u}$ are velocity and acceleration vectors; $\mathbf{P} = [P_1, \dots, P_i, \dots, P_n]^T$ is an external force vector; $\mathbf{1}$ is a diagonal one matrix; $\ddot{\mathbf{u}}_g = \begin{Bmatrix} \ddot{x}_g \\ \ddot{y}_g \end{Bmatrix}$ is ground acceleration; \mathbf{F}_{VFD} is a damping force vector generated by

VFD [4]. Element value of vector \mathbf{F}_{VFD} derives from equation(1).

2.2 Iterative solution of the P-Delta equation with SSA

Due mostly to P-Delta forces from beam-column elements of geometry nonlinearity, and damper forces generated from VFD, the differential equation (2) is defined only by numerical method at discrete time instants. By using the modified Newmark method, the time domain is discretized into constant time steps of t_i and t_{i+1} at every Δt . The response at the time instants t_{i+1} depends on not only applied loads but also the preceding quantities of axial forces of beam-column elements at the time t_i . Optimal location indices are calculated by means of root mean square values ($v_{\text{max}}^{\text{RMS}}$) of interstory drifts in velocities. The first damper is located where velocities are the greatest velocity values. After the stiffness and damping of first VFD are placed into mathematical model, the second VFD is then placed at the position where velocities are the greatest velocity values of the structure with the first VFD. The procedure is repeated for all necessary dampers. The numerical method for equation (2) is illustrated in Figure 3 with the helps of MATLAB routine.

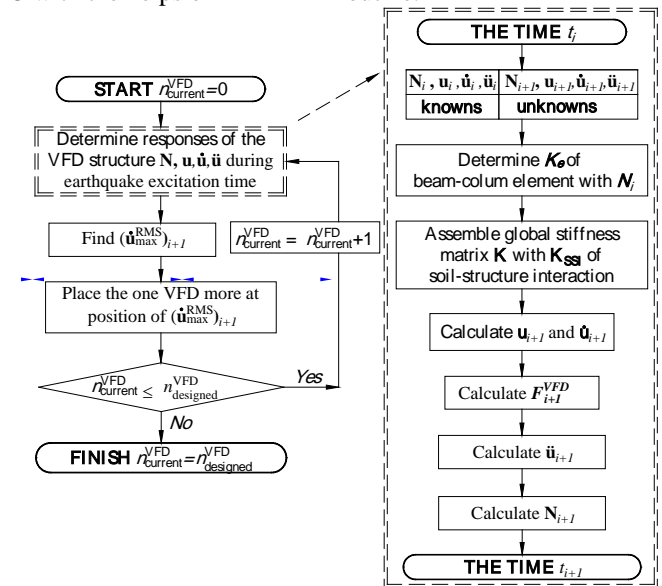


Figure 3: SSA algorithm of optimal configuration design for VFD structures considering the P-Delta effect and SSI

3. NUMERICAL EXAMPLES

The 20-story steel building [23] retrofitted with 20 VFD has yield strength $\sigma_y=345\text{MPa}$ and the damping ratios for two first modes of $\zeta_1=\zeta_2=2\%$. Its dynamic properties are given in Figure 5. The structure uses two pile foundations ① and ②.

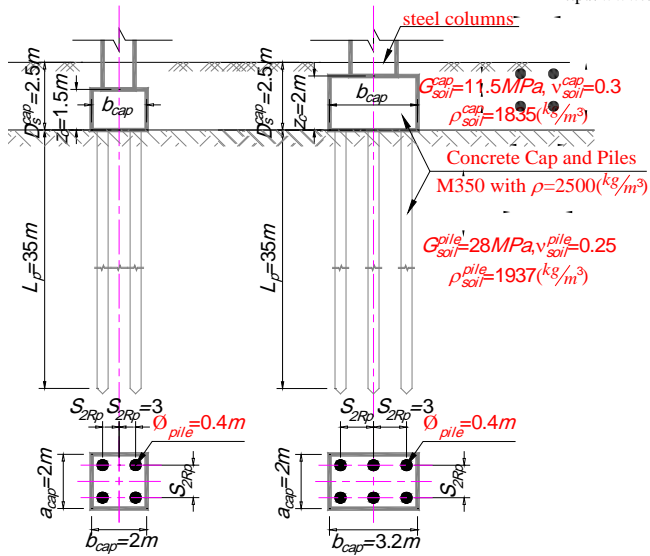


Figure 4: Pile foundations ① and ②

The diameter of all circular piles is $2R_p=0.4m$. The number of piles in foundation ② is $n_p = 2 \times 3 = 6$ with ratio of S

(distance between two piles) and $2R_p$ as $\frac{S}{2R_p} = 3$. The

dimension of foundation ① are the same as foundation ② but the number of piles in foundation ① is three and the distance between two piles are also S . Foundations ① are at exterior corner columns and foundations ② are at interior columns. The concrete grade of the foundations ① and ② is M350 (TCVN) [24] with $E_p=30GPa$.

Story	H_i (m)	Column	Beam	m_i ($\times 10^3$ kg)
1 st	5.49	W24x335	W30x99	563
2 nd	3.96	W24x335	W30x99	552
3 rd	3.96	W24x335	W30x99	552
4 th	3.96	W24x335	W30x99	552
5 th	3.96	W24x229	W30x108	552
6 th	3.96	W24x229	W30x108	552
7 th	3.96	W24x229	W30x108	552
8 th	3.96	W24x229	W30x108	552
9 th	3.96	W24x229	W30x108	552
10 th	3.96	W24x229	W30x108	552
11 th	3.96	W24x192	W30x99	552
12 th	3.96	W24x192	W30x99	552
13 th	3.96	W24x192	W30x99	552
14 th	3.96	W24x131	W30x99	552
15 th	3.96	W24x131	W30x99	552
16 th	3.96	W24x131	W30x99	552
17 th	3.96	W24x117	W27x84	552
18 th	3.96	W24x117	W27x84	552
19 th	3.96	W24x84	W24x62	552
20 th	3.96	W24x84	W21x50	584

Layer	Soil at pile cap					
	Height D_s^{cap} (m)	Young modulus E_s^{cap} (MPa)	Poisson coef f. ν_s^{cap}	Shear modulus G_s^{cap} (MPa)	Density ρ_s^{cap} (kg/m ³)	Soil velocity c_s^{cap} (m/s)
I	2.5	30.0	0.30	11.5	1835	79
Soil at piles						
II	35	70.0	0.25	28.0	1937	120

Therefore, mas, the stiffness and damping coefficients of foundation ② are [16][17][19][20][21][25] $m_0^{\circ} = 32000kg$,

$$k_x^{\circ} = 5.735 \times 10^5 \text{ kN/m}, c_x^{\circ} = 7.422 \times 10^3 \text{ kN.s/m},$$

$$k_y^{\circ} = 24.387 \times 10^5 \text{ kN/m}, c_y^{\circ} = 7.204 \times 10^3 \text{ kN.s/m},$$

$$k_{\theta}^{\circ} = 230.890 \times 10^5 \text{ kN/m}, c_{\theta}^{\circ} = 72.040 \times 10^3 \text{ kN.s/m};$$

and of foundation ① are $m_0^{\circ} = 15000kg$,

$$k_x^{\circ} = 4.727 \times 10^5 \text{ kN/m}, c_x^{\circ} = 5.614 \times 10^3 \text{ kN.s/m},$$

$$k_y^{\circ} = 24.387 \times 10^5 \text{ kN/m}, c_y^{\circ} = 7.204 \times 10^3 \text{ kN.s/m},$$

$$k_{\theta}^{\circ} = 76.105 \times 10^5 \text{ kN/m}, c_{\theta}^{\circ} = 26.147 \times 10^3 \text{ kN.s/m}$$

http://www.ejournalofscience.org

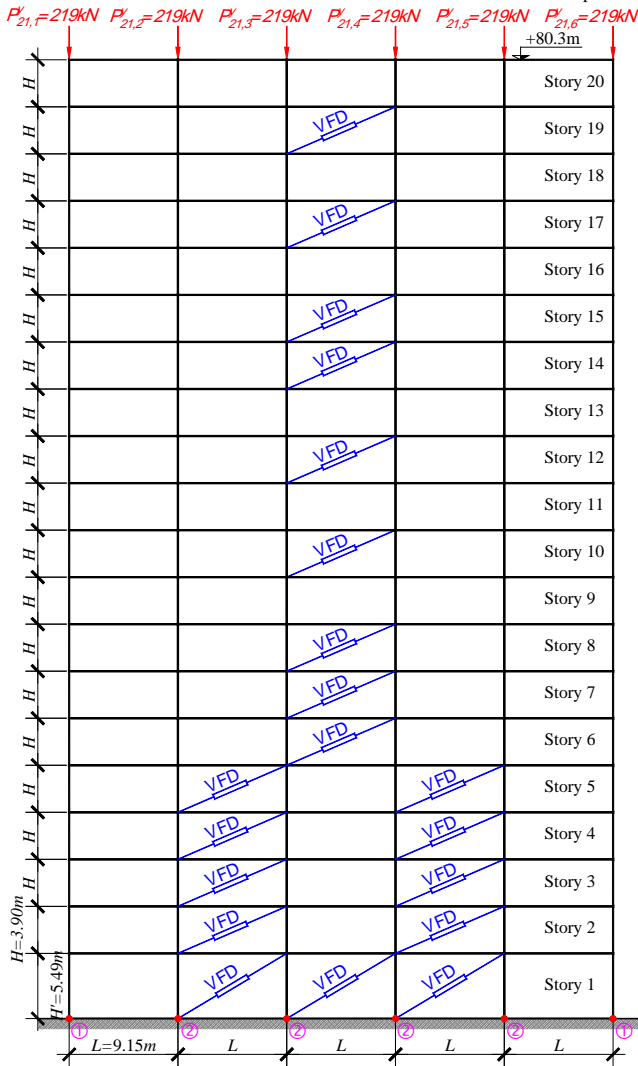


Figure 5: The benchmark 20-story building with 20 VFD at optimal configuration

Table 1: Analyzed Cases

	Name of cases	Analysis combined				
		Linear	P-Δ	SSI	VFD uni.	VFD opt.
VFD Control	(LIN without SSI) _{NCT}	✓				
	(LIN with SSI) _{NCT}	✓		✓		
	(P-Δ without SSI) _{NCT}		✓			
	(P-Δ with SSI) _{NCT}		✓	✓		
VFD Controlled	(LIN without SSI) _{VFD,uni}	✓			✓	
	(LIN without SSI) _{VFD,opt}			✓		✓
	(LIN with SSI) _{VFD,uni}	✓		✓	✓	
	(LIN with SSI) _{VFD,opt}	✓		✓		✓
	(P-Δ without SSI) _{VFD,uni}		✓		✓	
	(P-Δ without SSI) _{VFD,opt}		✓			✓
	(P-Δ with SSI) _{VFD,uni}		✓	✓	✓	
	(P-Δ with SSI) _{VFD,opt}		✓	✓		✓

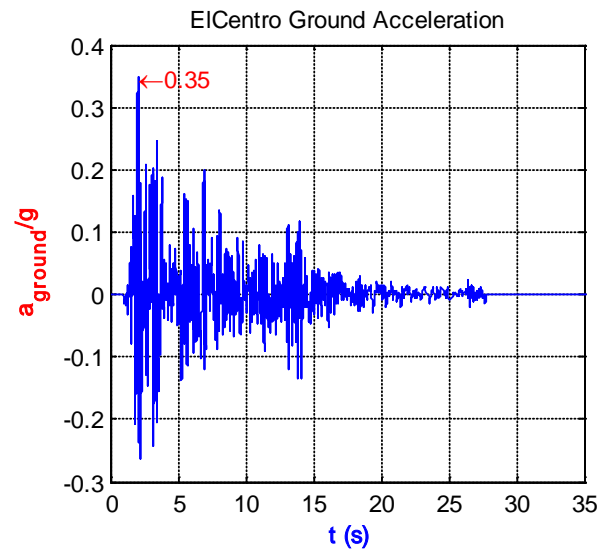


Figure 6: Time history of the ElCentro ground acceleration [3]

The first three natural periods of the linear structure are $T_1 = 2.08s$; $T_2 = 0.73s$; and $T_3 = 0.42s$; the periods of the structure considering both the geometry nonlinearity structures and its SSI are $T_1 = 2.13s$; $T_2 = 0.74s$; and $T_3 = 0.43s$. On the roof there are five vertically external forces of $219kN$ acting on the VFD structure.

The ElCentro earthquake [3] acts on the building along the x axis with peak ground acceleration (PGA) of $(\ddot{x}_g)_{max} = 0.35g$ (Figure 6). Analysis duration is 35 seconds with constant time intervals of $\Delta t = 0.00125s$.

The response of the structure are analyzed into two groups of non-controlled and VFD controlled structures as Table 1. With VFD optimally controlled, their positions are shown in Figure 5 [26][27] and the VFD control parameters in one

$$\text{portal are taken as } \begin{cases} C_j^{VFD} = 2 \times 10^6 \text{ Ns/m}; \alpha_j = 1 \\ f_{j,max}^{VFD} = 120kN \end{cases}$$

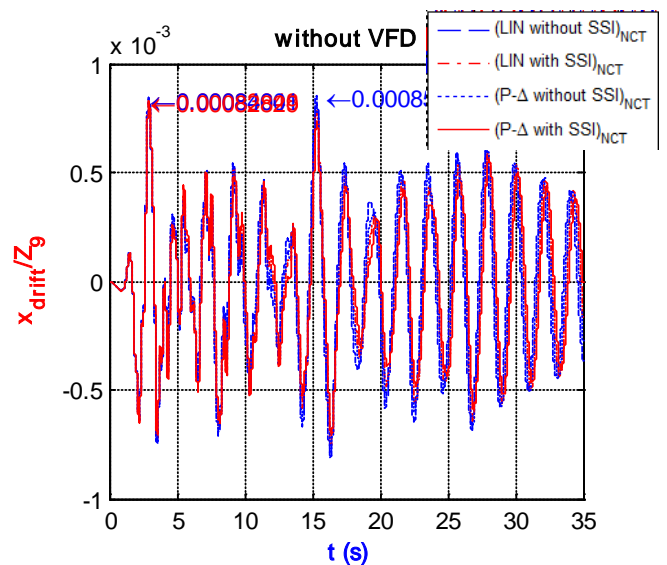


Figure 7: Story drift response versus time without VFD

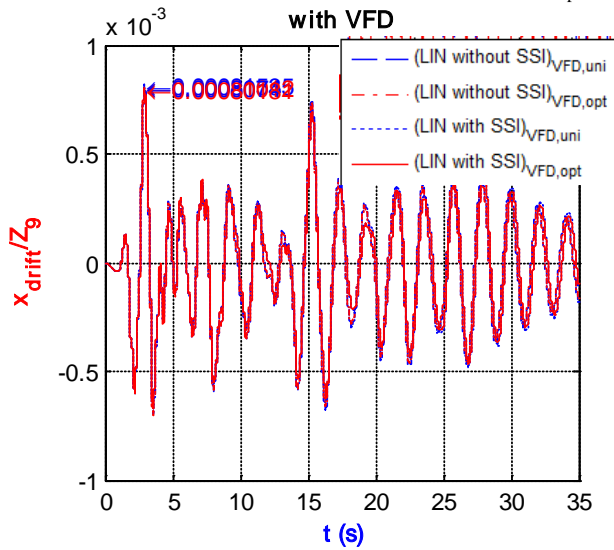


Figure 8: Story drift response versus time with VFD in the linear analysis

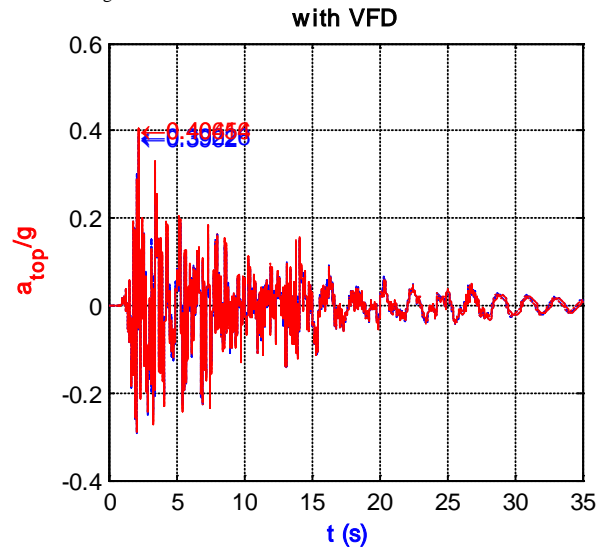


Figure 11: Top acceleration response versus time with VFD in the linear analysis

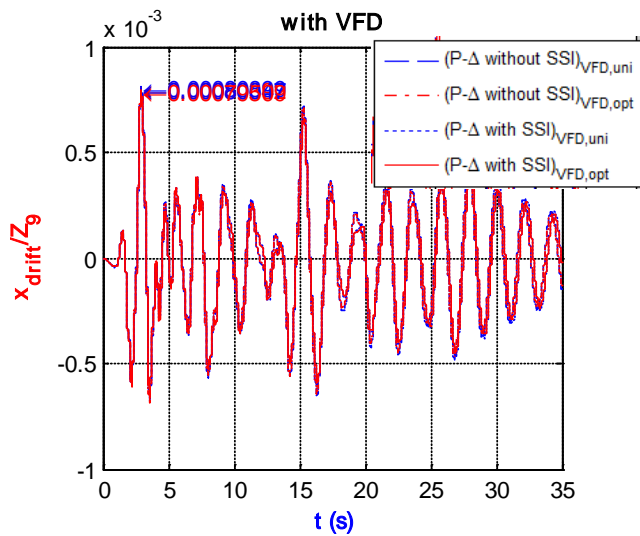


Figure 9: Story drift response versus time with VFD in the P-Δ analysis

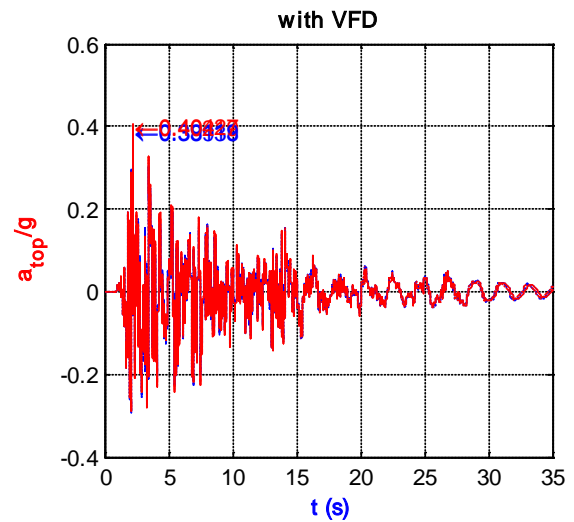


Figure 12: Top acceleration response versus time with VFD in the P-Δ analysis

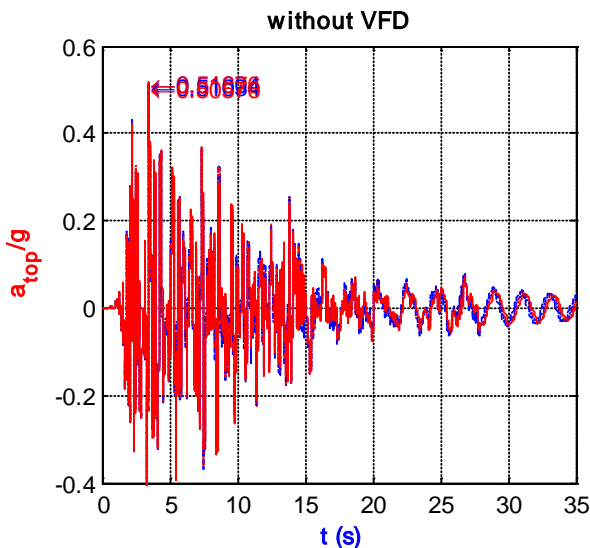


Figure 10: Top acceleration response versus time without VFD

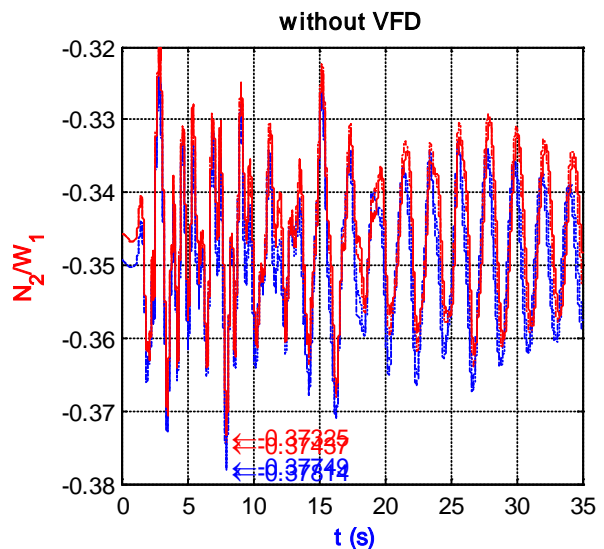


Figure 13: Axial force of the second column without VFD

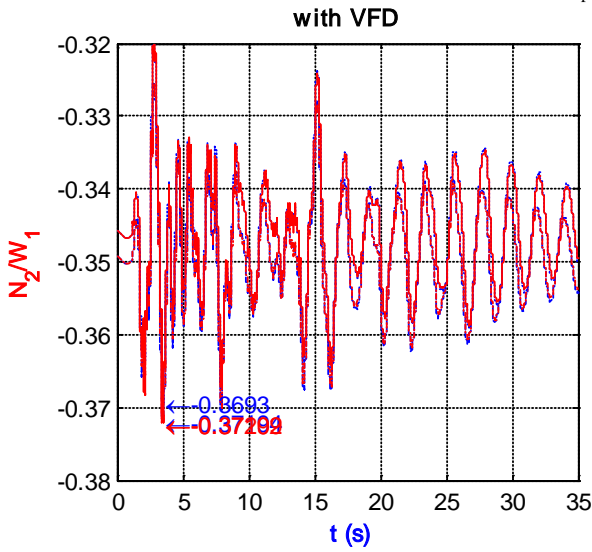


Figure 14: Axial force of the second column with VFD in the linear analysis

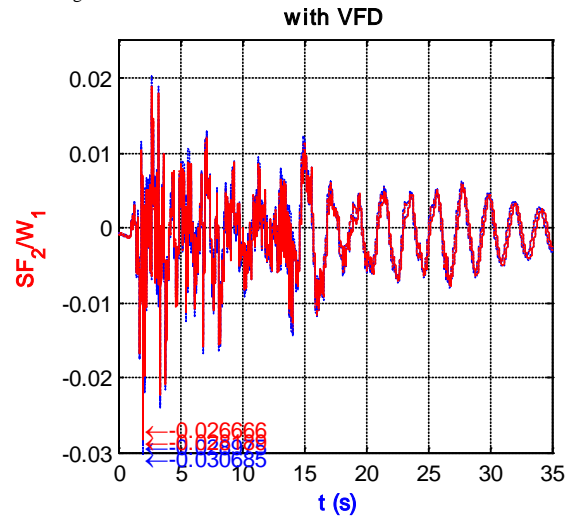


Figure 17: Shear force at the end a of the second column with VFD in linear analysis

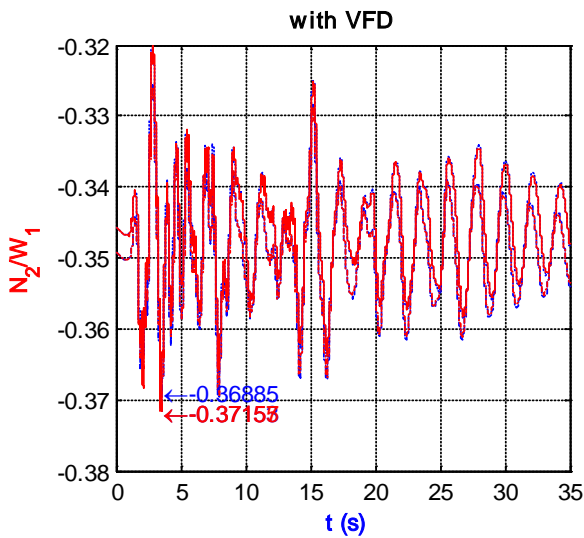


Figure 15: Axial force of the second column with VFD in the P-Δ analysis

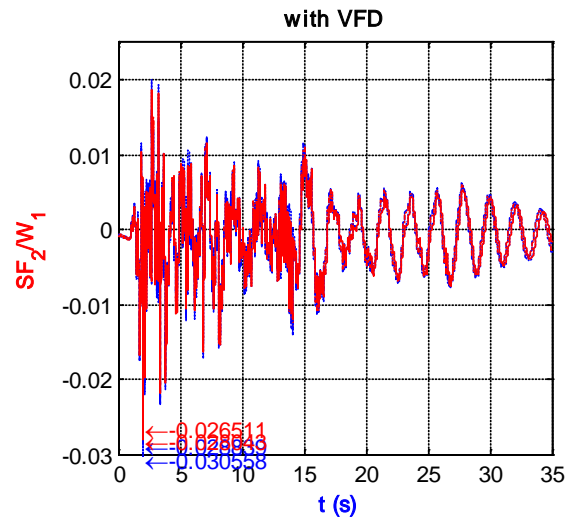


Figure 18: Shear force at the end a of the second column with VFD in P-Δ analysis

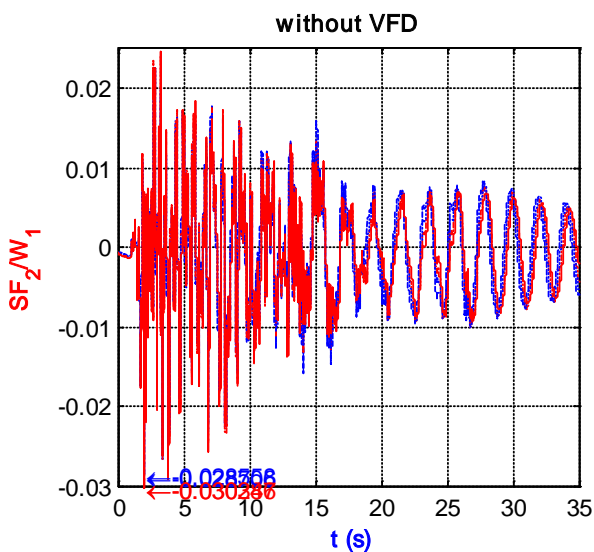


Figure 16: Shear force at the end a of the second column without VFD

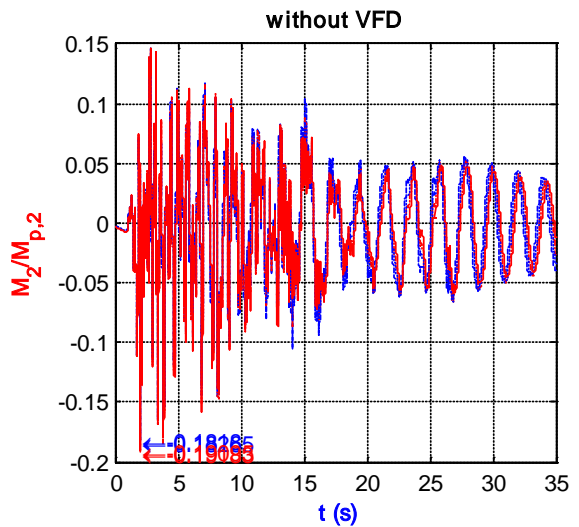


Figure 19: Moment at the end a of the second column ($M_{p,2} = W_{p,2} \cdot \sigma_y^{col}$) without VFD

http://www.ejournalofscience.org

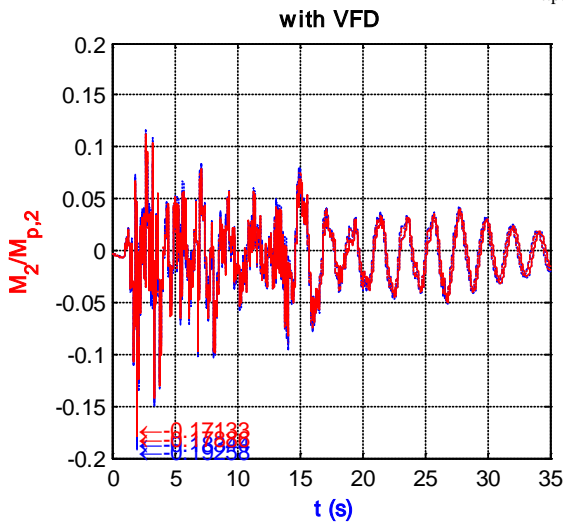


Figure 20: Moment at the end a of the second column ($M_{p,2}=W_{p,2} \cdot \sigma_y^{col}$) with VFD in P-Δ analysis

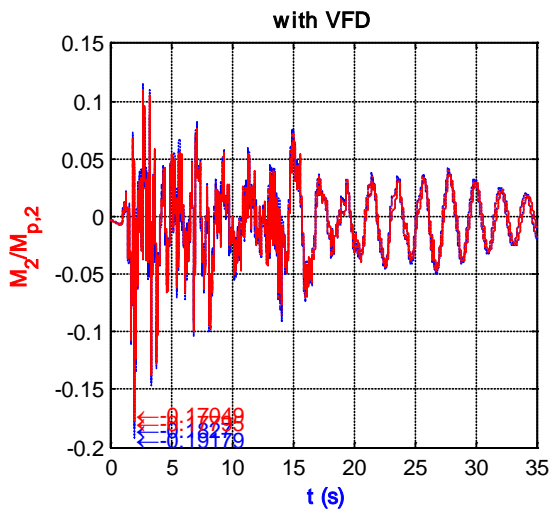


Figure 21: Moment at the end a of the second column ($M_{p,2}=W_{p,2} \cdot \sigma_y^{col}$) with VFD in P-Δ analysis

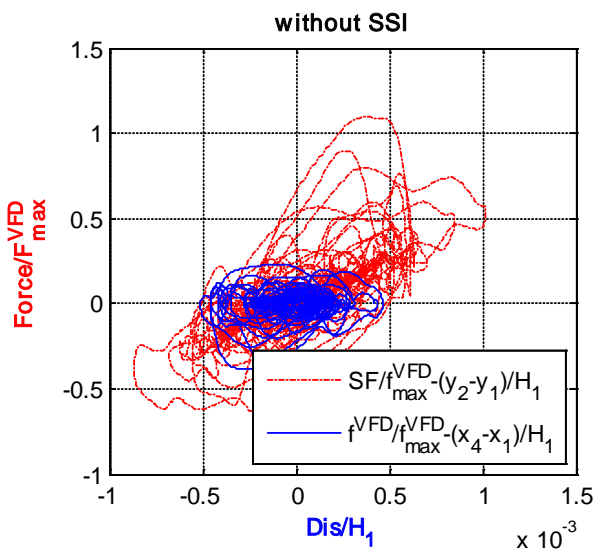


Figure 22: Hysteretic loop of Shear force and VFD without SSI

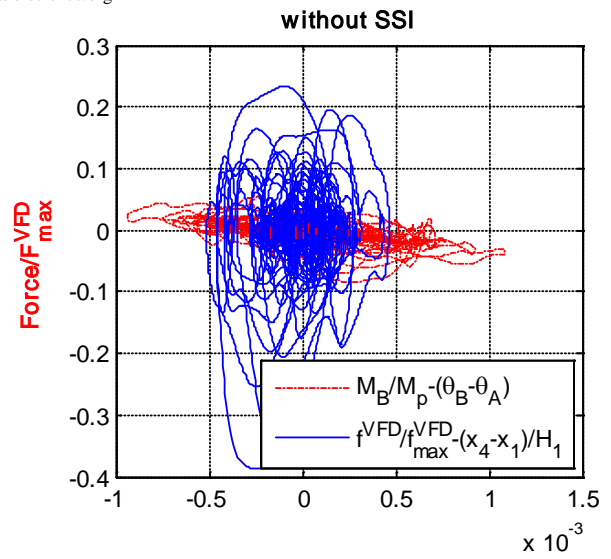


Figure 23: Hysteretic loop of Moment and VFD without SSI

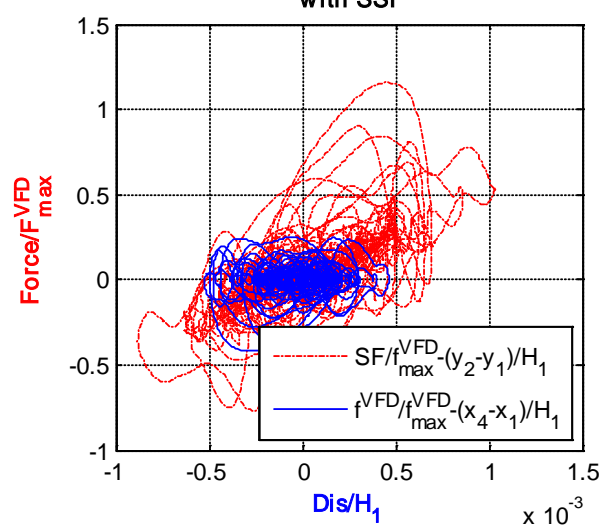


Figure 24: Hysteretic loop of Shear force and VFD with SSI

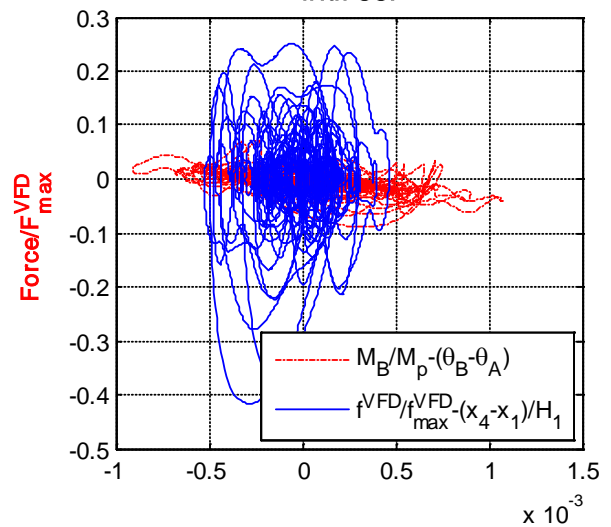


Figure 25: Hysteretic loop of Moment and VFD with SSI

<http://www.ejournalofscience.org>

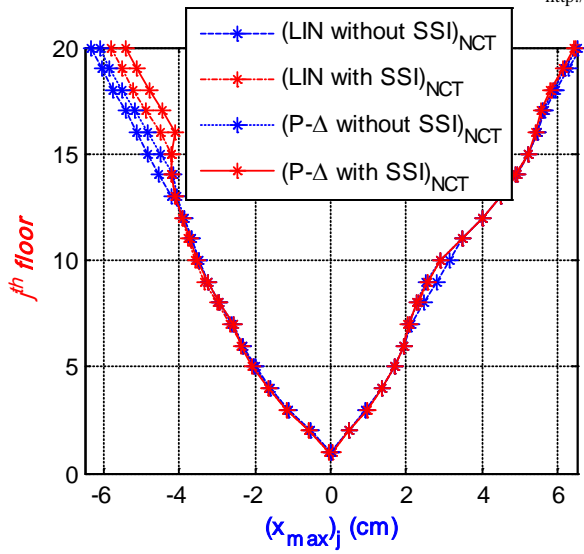


Figure 26: Maximum story drift without VFD

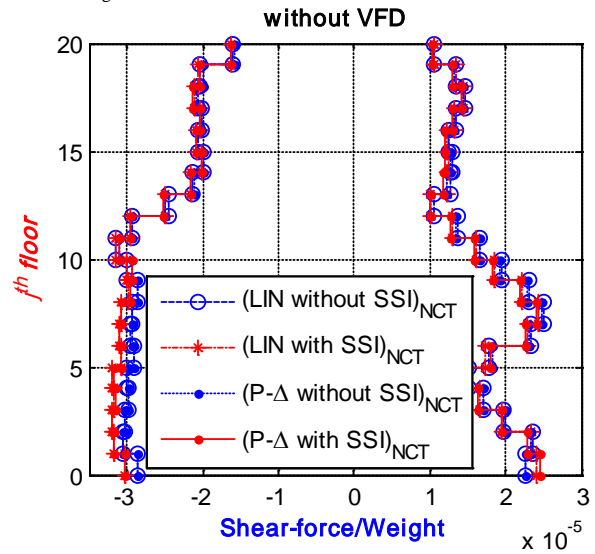


Figure 29: Ratio of columns' maximum shear forces at 1-axis to its weight without VFD

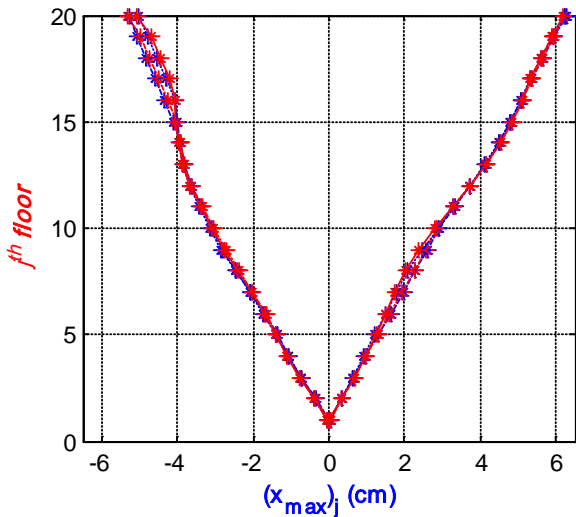


Figure 27: Maximum story drift with VFD in linear analysis

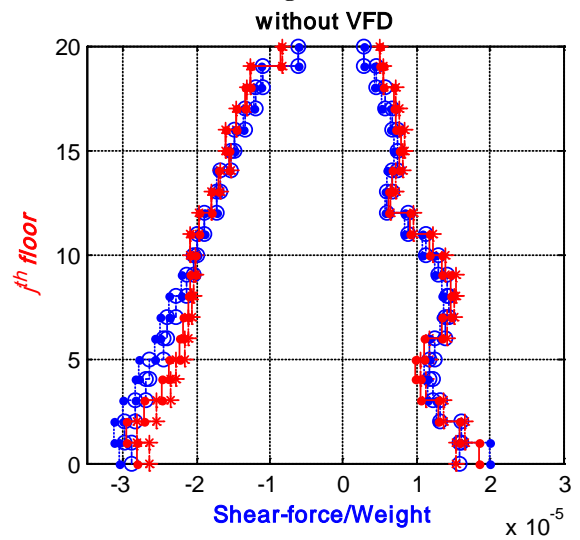


Figure 30: Ratio of columns' maximum shear forces at 1-axis to its weight with VFD

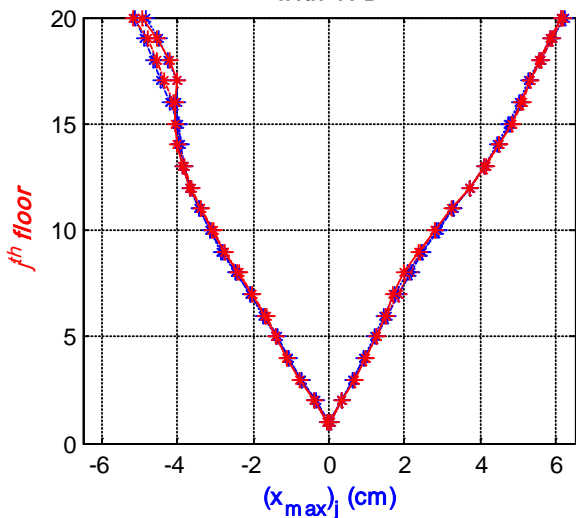


Figure 28: Maximum story drift with VFD in P-Δ analysis

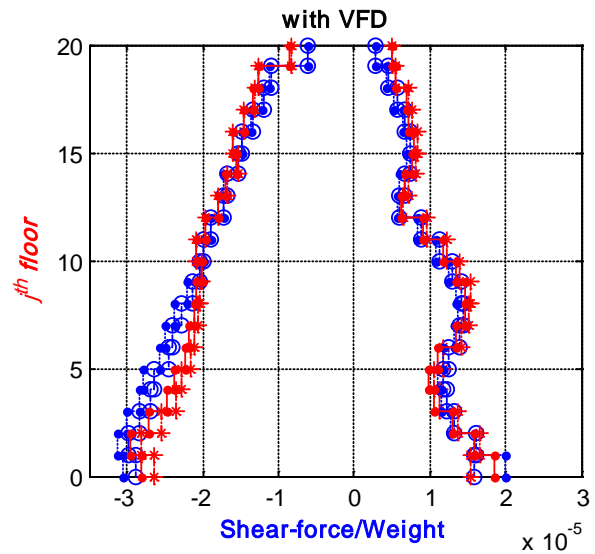


Figure 31: Ratio of columns' maximum shear forces at 1-axis to its weight with VFD

http://www.ejournalofscience.org

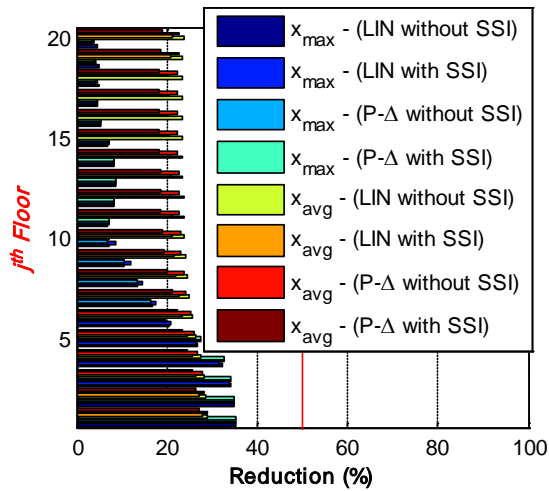


Figure 32: Dynamic reduction in horizontal displacements and accelerations with and without SSI in uniform VFD

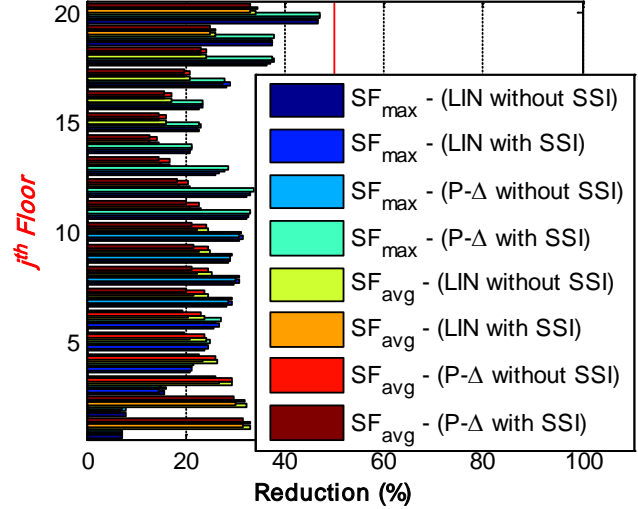


Figure 35: Dynamic reduction in Shearforce at column ends with and without SSI in optimal VFD

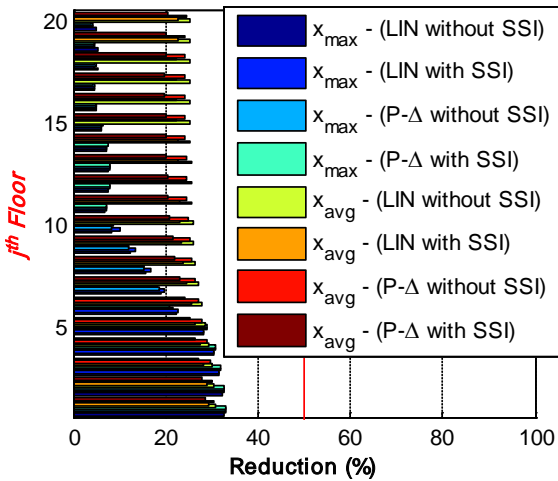


Figure 33: Dynamic reduction in horizontal displacements and accelerations with and without SSI in optimal VFD

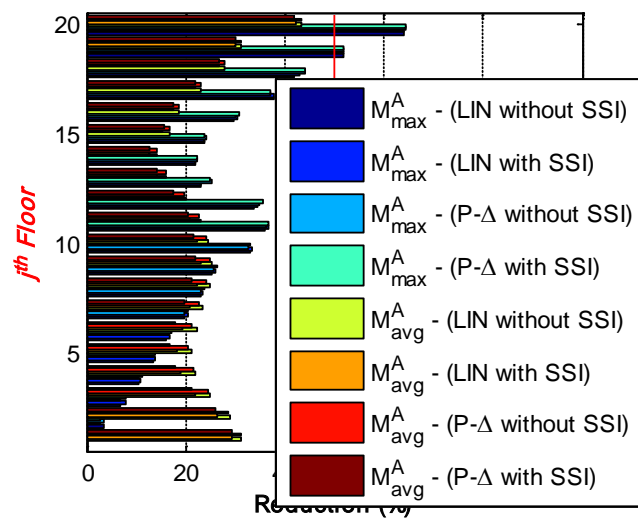


Figure 36: Dynamic reduction in Moment at column ends with and without SSI in uniform VFD

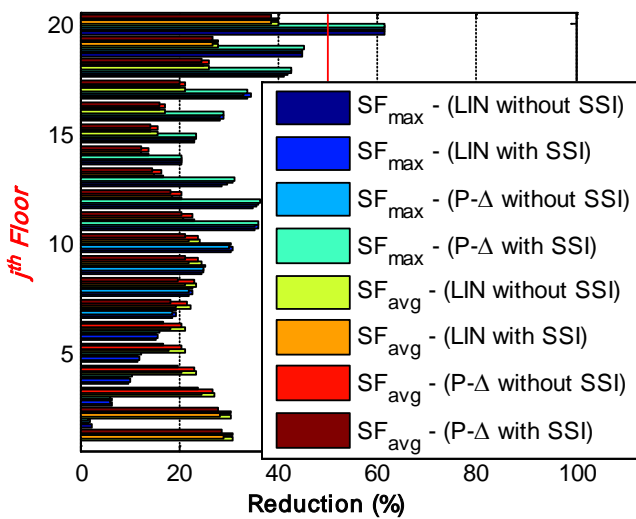


Figure 34: Dynamic reduction in Shear force at column ends with and without SSI in uniform VFD

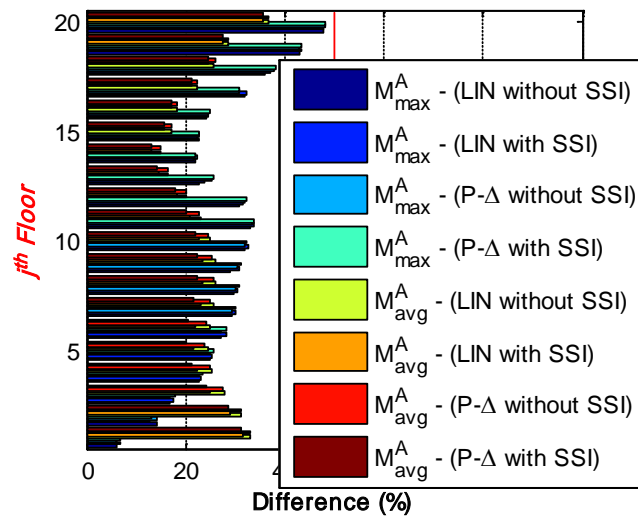


Figure 37: Dynamic reduction in Moment at column ends with and without SSI in optimal VFD

<http://www.ejournalofscience.org>

Moment internal forces at column end A is absolutely lesser than its moment plastic resistance $M_{p,2}$, proving reasonability of linear and P- Δ dynamic analysis in the paper. There is no acceleration after 27 seconds (Figure 6), however dynamic responses has not decayed immediately (Figure 7 to Figure 21) due to a less amount of damping ratio of the structure.

In all cases dynamic responses such as displacement, shearforce, and moment at column ends are compared in Figure 7 to Figure 37. Without VFD and Non-SSI and SSI analysis, the difference of maximum shear force values on each of the story is $121.65\%/20=6.08\%$. Compared to linear analysis and Non-SSI in case of no VFD, both P- Δ and SSI analysis shows in each of the floors 2% and 9% differences for maximum and average displacement respectively; 3% for both maximum and average shear force and moment.

For dynamic response reduction of VFD for the 20 story building, the difference between VFD uniform placement and optimal placement is not much, approximate 527.7% vs 561.8% respectively for M_{avg}^A in SSI and P- Δ analysis.

Compared to VFD uniformly placed in cases of SSI vs Non-SSI analysis, the difference of VFD optimally placed is greater than 10.6% (488.1% compared to 441.3%) and its reductions in shear force and moment are equally distributed in each of the floors (Figure 34 vs Figure 35, Figure 36 vs Figure 37). The reduction in dynamic response amplitude is strongly dependent on VFD. Hence, the dynamic response reduction in P- Δ and SSI analysis can be improved by employing more VFD rather than increasing f_{VFD}^{\max} because of $f_{VFD} / f_{VFD}^{\max} < 1$,

VFD not fully in specific damping capacity (Figure 23 to Figure 25). Moreover, the effect of P- Δ on dynamic responses can be clearly higher if the columns are subjected to more axial loads.

4. CONCLUSION

This paper presents dynamic analysis of the 20-story VFD structures considering soil-structure interaction, P- Δ effects, and subjected to seismic loading. The reasonable result is proved through the numerical example and its plastic moment resistance. Numerical results with helps of MATLAB codes in the case of dynamic analysis are compared each other. Compared to VFD uniformly placed, the responses of VFD optimally placed are slightly higher than approximate 10%. Twenty VFD significantly reduces the response of the 20-story building by using VFD optimal configuration. This effectiveness of VFD could be demonstrated via non-linearity of steel material behavior and other seismic loadings. The more addition of VFD, the higher reductions in response are achieved.

ACKNOWLEDGEMENT

This research is funded by International University, VNU-HCM under grant number T2016-01-CE.

REFERENCES

[1] Bathe, K.-J., Finite Element Procedures in Engineering Analysis, Prentice Hall, Englewood Cliffs, NJ., 1982.

- [2] Anil K. Chopra (2012), "Dynamics of Structures", 4th edition, Prentice Hall Press.
- [3] <http://www.vibrationdata.com>
- [4] Robert J. McNamara and Douglas P. Taylor (2003), "Fluid viscous dampers for high-rise buildings", the structural design of tall and special buildings, Vol.12, pp.145–154, <http://taylordevices.com/literature.html>
- [5] Douglas P. Taylor, Israel Katz (2004) – Seismic protection with fluid viscous dampers for the Torre Mayor, a 57-story office tower in Mexico City, Mexico, <http://taylordevices.com/literature.html>
- [6] Chan, Siu-Lai, and Pui-Tak Chui, Non-linear static and cyclic analysis of steel frames with semi-rigid connections. Elsevier, 2000
- [7] Kim, Seung-Eock, Moon-Ho Park, and Se-Hyu Choi. Direct design of three-dimensional frames using practical advanced analysis. Engineering Structures 23.11 (2001): 1491-1502.
- [8] Kim, Seung-Eock, Practical second-order inelastic analysis for steel frames subjected to distributed load. Engineering Structures 26.1 (2004): 51-61.
- [9] Seung-Eock Kim, Cuong Ngo-Huu, Dong-Ho Lee, Second-order inelastic dynamic analysis of 3-D steel frames. International Journal of Solids and Structures 43 (2006) 1693–1709.
- [10] Liew, J. Y. R. Advance analysis for frame design. PhD dissertation, Purdue Univ., West lafayette, Ind, 1992.
- [11] Liew, J. Y. R., White, D. W., and Chen, W. F., Second-order refined plastic hinge analysis for frame design: Part II. J. Struc Engrg., ASCE, 119(11),3217-3237.
- [12] Chandrakant S.Desai, Musharaf Zaman – Advanced Geotechnical Engineering, CRC Press Taylor & Francis Group, 2014.
- [13] T. K. Datta, Seismic analysis of structures – Indian Institute of Technology Delhi, India, 2010.
- [14] Sandro Carbonari, Francesca Dezi, Graziano Leoni – Linear soil-structure interaction of coupled wall–frame structures on pile foundations, Elsevier Ltd, 2011.
- [15] Milos Novak – Dynamic Stiffness and Damping of Piles. Canadian Geotechnical Journal, 1974.
- [16] M. Shadlou and S. Bhattacharya – Dynamic stiffness of pile in a layered elastic continuum. S. Geotechnique, 2014.
- [17] Amir M. Kaynia – Dynamics of piles and pile groups in layered soil media. Soil Dynamics and Earthquake Engineering, 1991.
- [18] George Gazetas and Ricardo Dobry – Horizontal response of piles in layered soils. Journal of GeotechnicalEngineering, 1984.
- [19] M.C. Constantinou, M.D. Symans (1993), "Experimental study of seismic response of buildings

<http://www.ejournalofscience.org>

with supplemental fluid dampers”, The structural Design of tall buildings, pp. 93-132.

- [20] Y.Ohtori, R. E. Christenson, B. F. Spencer (2004), “Benchmark Control Problems for Seismically Excited Nonlinear Buildings”, Journal of Engineering Mechanics © ASCE / April 2004.
- [21] TCXDVN 338:2005 about Steel Structure - Design Standard,
<http://www.xaydung.gov.vn/web/guest/english>
- [22] Dang Van Ut, Pham Nhan Hoa, Chu Quoc Thang, “Analysis of a story steel building accompanied with its pile foundation considering soil-structure interaction subjected to seismic loading”, Construction National Journal, 7-2016, pp. 72-78
- [23] Pham Nhan Hoa, Chu Quoc Thang, “Configuration Optimum for Viscous Fluid Dampers in General Approach”, ARPN Journal of Science and Technology, March 2016, pp. 96-102
- [24] Pham Nhan Hoa, Chu Quoc Thang, Ong Hoang Truc Giang, “Optimal placement of viscous fluid dampers for building seismic resistance”, ARPN Journal of Science and Technology, August 2015, pp. 377-388.
- [25] Diego Lopez Garcia, M.EERI, “A Simple Method for the Design of Optimal Damper Configurations in MDOF Structures Diego Lopez Garcia, M.EERI”, Earthquake Spectra. Volume 17, No. 3. August 2001.

AUTHOR PROFILES

PHAM NHAN HOA received the master degree in computational civil engineering from Liege, Belgium in 2006. Currently, he is now a lecturer at International University – Vietnam National University, Vietnam.

CHU QUOC THANG received the PhD degree in structural engineering from TTI, Hungary in 1987. Currently, he is an Associate Professor at International University – Vietnam National University, Vietnam.

DUY received his master degree in civil engineering from Ho Chi Minh University of Technology in 2014. Currently, he is a lecturer at Quy Nhon University – Vietnam.